Analyses of Seismic Slope Stability and Subsequent Debris Flow Modeling

Analysis de stabilité de pente sous sollicitation sismique et modélisation des écoulements de boues induits

Long X., Tjok K.-M.
Fugro GeoConsutling Inc., Houston, Tx

ABSTRACT: Earthquake-triggered slope failures and subsequent submarine debris mass flow can cause severe consequences and jeopardize the integrity of offshore structures in the proximity. In this paper, a two-dimensional seismic slope stability analysis for an offshore liquefied slope site located in American Petroleum Institute (API) seismic zone 4 with layered stratigraphy is addressed. A nonlinear dynamic analysis using the stress-strain law of "hysteretic modeling" allowing for soil weakening under large strains was adopted to study flow failure instability. Laboratory tests were performed for the derivation of soil dynamic parameters and calibration of hysteretic soil model. Using "Constant-volume" constraints, the run-out distance of subsequent debris flow was also estimated.

RÉSUMÉ : Lors de séismes, les ruptures de pentes et les écoulements (de boue) sous-marin qui s'en suivent peuvent avoir des conséquences graves et compromettre l'intégrité des structures « offshore » voisines. Dans cet article, on présente une étude (2D) de stabilité d'une pente dans un site « offshore » liquéfiable, dans un zone sismique de niveau 4 (référentiel de l'American Petroleum Institute). Une analyse dynamique non-linéaire utilisant la loi « hysteretic modeling » (loi permettant la modélisation du radoucissement en grande déformation) a été adoptée pour étudier la rupture des pentes et les écoulements induits. Des tests de laboratoire ont été effectués afin d'identifier et de déterminer les paramètres numériques de la loi de comportement. En se plaçant dans le cadre des déformations à volume constant, la modélisation a permis d'estimer la distance parcourue par les écoulements de boues.

KEYWORDS: earthquake slope debris flow non-linear dynamic.

1 INTRODUCTION

Earthquakes are one of the major casuses of submarine slides. Large shear stresses and deformations may be generated due to seismic vibrations and irrecoverable volume changes are accumulated accompanied by the rise of pore water pressure (i.e., decrease of effective stress) and cyclic degradation of shear strength. Liquefaction occurs when the effective stress equals zero and soil behaves as a liquid. The submarine debris mass flow following the onset of liquefaction and instablity of liquefied slope can pose significant impact force and thus jeopardize the integrity of offshore structures in the flow path.

In this paper, a two-dimensional seismic submarine slope stability analysis is performed using commercial computer program FLAC (***F***ast ***L***agrangian ***A***nalysis of ***C***ontinua) (Itasca, FLAC 7.0, an explicit finite difference program operating in the time domain. It simulates the behavior of soils which may subject to plastic flow when their yield limits are reached. The Finn Model- Byrne Formulation is implemented in the analysis to assess dynamic pore pressure generation and liquefaction potential. Based on "constant-volume" constraints, the run-out distance of subsequent debris flow was predicted using the one-dimensional subagqueous debris flow model BING (Imran and Parker, 2001).

2 TWO-DIMENSIONAL NON-LINEAR DYNAMIC ANALYSIS

The slope stability and liquefaction potential for a project site under seismic loading is assessed using FLAC for a two-dimensional non-linear dynamic analysis. The dynamic stress-strain behavior for the soil layers are simulated using a hysteretic model by means of a non-linear stress-strain back bone curve and the associated stress-strain loops that represent the energy dissipated in the soil during seismic loading. Strain-controlled cyclic simple shear tests have been performed to determine dynamic soil parameters and calibration of hysteretic soil model.

2.1 Site Condition

The site is located in International Organization for Standardization (ISO) seismic zone 4 (ISO 2004). Soil stratigraphy consists of soft to firm clay layers overlying dense fine sand. Based on the in situ suspension P (compression wave velocity)-S (shear wave velocity) logging and cone penetration test (CPT) data, the upper 33m (100ft) of the effective seabed is around 160 m/s (525 ft/s) and the site is classified as either American Petroleum Institute (API) criteria Type C or ISO criteria Type E.

Figure 1 below illustrates the soil strategraphy at the study site. The subsurface conditions comprise of 50 m (160 ft) soft to firm clay underlain by a layer of dense to very dense fine sand down to 105 m (350 ft). The mean sea level is 61.0 m (200 ft) above seafloor. Due to soil erosion, a 20˚ slope is formed as detected from the geophysical multibeam bathymetric data. In light of variations of material parameters, three soil Strata, i.e., Stratum I , II and III, respectively, are defined within the clay sediment. For the study of effective stress analysis, four Strata with Stratum I, II and III for cohesive materials and Stratum IV for cohesionless sediment, are used. The soil parameters including submerged unit weight γ, average shear wave velocity V_s, cohesion c, and friction ϕ for each stratum are also provided on the figure. .

The laboratory test data from cyclic direct simple shear (CDSS) along with the generic curves of similar soil types (Seed & Idriss for sand) were used as guidance to develop hysteretic model for the analysis. Figure 2 presents the dynamic

soil characteristics used in the model as defined by the shear modulus degradation (G/Gmax) and damping ratio (D) curves.

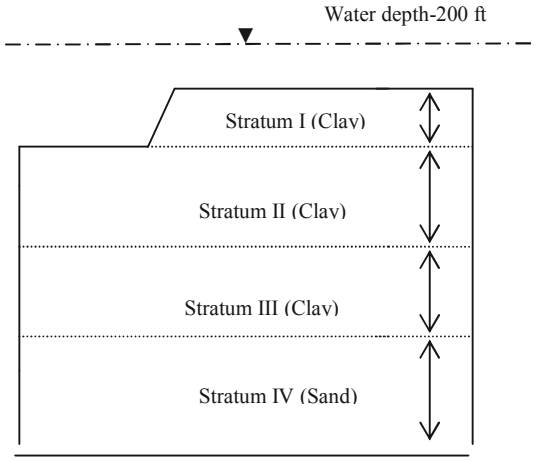

Stratum	Soil Parameters for Effective Stress Analysis
I (4.3m (14ft) thick)	γ=726 kg/m^3,Vs=122 m/s, c=4.8 kPa, ϕ=15^o
II (21.3m (70ft) thick)	γ=807 kg/m^3,Vs=186 m/s, c=5.8 kPa, ϕ=20^o
III (23.5m (76ft) thick)	γ=888 kg/m^3,Vs=300 m/s, c=5.8 kPa, ϕ=20^o
IV (58.0m (190ft) thick)	γ=1000 kg/m^3,Vs=335 m/s, ϕ=35^o

Figure 1. Soil stratigraphy for the study site (Not to scale).

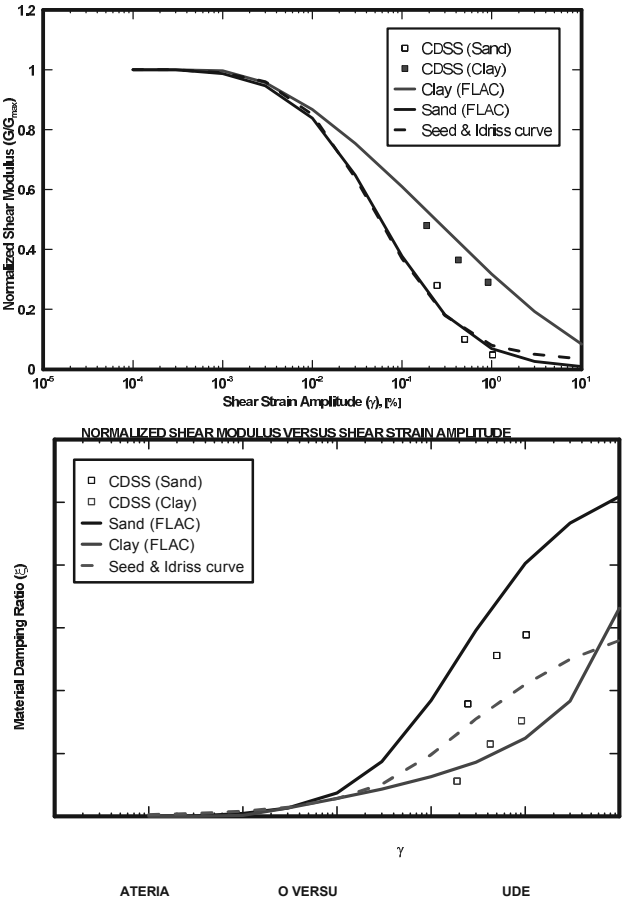

Figure 2. Soil dynamic characteristic curves

2.2 *Characteristic of Earthquake Input Motion*

The peak ground acceleration (PGA) of the earthquake motion is 0.48 g with a duration time of 40 sec. As indicated from the power spectra of input velocity and input acceleration as shown on Figure 3, the highest frequency component of the input motion is less than 10 Hz with the majority of the frequencies are less than 6 Hz. The input motion is applied at the depth of 105m (350ft).

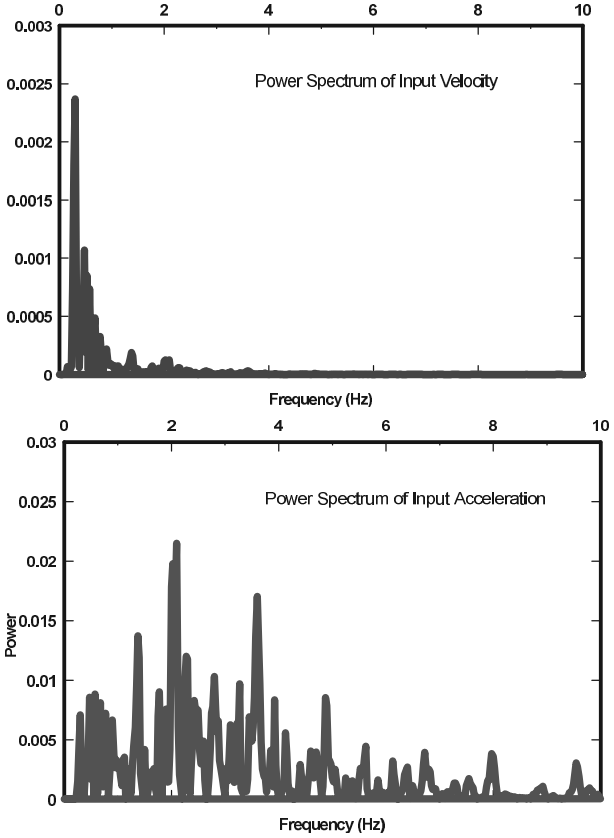

Figure 3. Acceleration time history and power spectrum of input motion.

2.3 *Two-Dimensional Numerical Modeling*

Kuhlemeyer and Lysmer (1973) state that for accurate representation of wave transmission through a model, the spatial element size, Δl, must be smaller than approximately one-tenth to one-eighth of the wavelength associated with the highest frequency component of the input wave, i.e., $\Delta l \leq \lambda/10$, or $f \leq Cs/(10\Delta l)$, where λ is the wavelength associated with the highest frequency component that contains appreciable energy; and Cs is speed of propagation associated with the mode of oscillation. Since the majority of the frequencies of input motion are less than 6.0 Hz, a 1.83m (6ft) x 1.83m (6ft) mesh size is selected for the modeling. The maximum frequency that can be modeled accurately for this element size is 6.7 Hz. The frequency of Dynamic excitation to the FLAC model was specified using the compliant-base deconvolution procedure (Mejia and Dawson, 2006). The input excitation was specified as a stress time history at the base of the model as a function of mass density ρ, shear wave velocity Vs at the half-space depth (105 m (350 ft) below seafloor) and input shear particle velocity v. Figure 4 demonstrates the FLAC mesh with rectangular and triangle shapes for this two-dimensional analysis. The free-field on vertical sides and quiet boundary conditions at the bottom are applied in the soil domain.

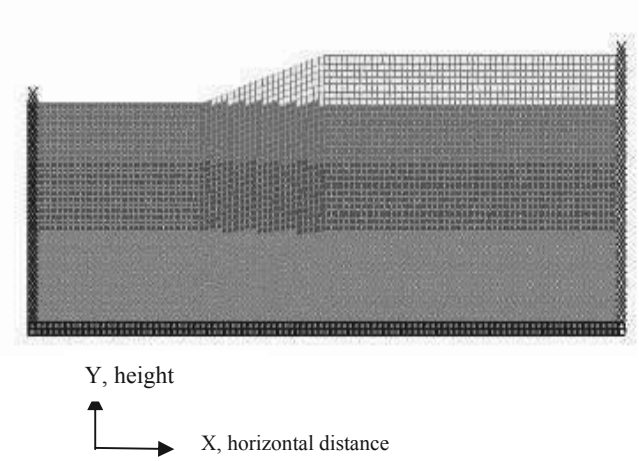

Figure 4. FLAC model for the modeling

The static equilibrium state at the time of the earthquake event is established to obtain the initial shear-stress distribution of the soil mass. The preliminary analysis, assuming undamped elastic-material, was performed to estimate maximum levels of cyclic shear strains and velocity levels throughout the model during the dynamic excitation. The maximum shear strain contour from the preliminary run is shown on Figure 5 indicating that the maximum elastic shear strains are smaller than 0.7 % throughout almost the entire modeled area. This range of shear strains is considered appropriate for inclusion of hysteretic damping based upon the dynamic characteristics of the soils as illustrated on Figure 2. The frequency range for the natural response of the elastic materials is calculated to be relatively uniform throughout the model, with a dominant frequency of approximately 3 Hz.

A fully coupled nonlinear seismic analysis is performed using the Mohr-Coulomb model to represent the soil layers, with additional hysteretic damping applied to simulate the non-linear soil dynamic behavior. Due to the fact that hysteretic damping does not completely damp high frequency component, a small amount of stiffness-proportional Rayleigh damping is also employed in the analysis.

The Finn-Byrne model is used for the liquefaction simulation by considering Strata I and II as liquefiable materials. Based on CPT/SPT correlations from in-situ CPT data and fine contents (Kulhawy and Mayne, 1990), the equivalent normalized SPT blow counts are assigned for the two strata. The automatic rezoning logic is applied in the analysis to correct for severely distorted mesh conditions developed during the simulation of earthquake shaking. The onset of liquefaction is identified by the cyclic pore-pressure ratio, u_e/σ_c', where u_e is the excess pore pressure and σ_c' is the initial in-situ effective confining pressure. After the liquefaction, the soil shear strength is reduced to residual strength which is 30% of the original value.

The numerical analysis indicates the development of liquefaction and failure surface in the slope. Figure 6 displays the contours of maximum shear strain at the end of earthquake excitation (40 seconds). The contour of excess pore pressure ratio equaling 1 (onset of liquefaction) at 40 seconds is also marked in green line on Figure 6. Figure 7 shows the vertical and horizontal displacement histories at the slope crest. The negative sign for X and Y axes indicate the left direction and downward direction, respectively. the slope moves horizontally approximately 8.5m.

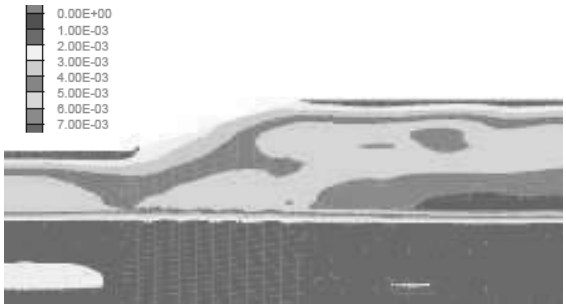

Figure 5. Maximum shear strain contours from undamped elastic analysis

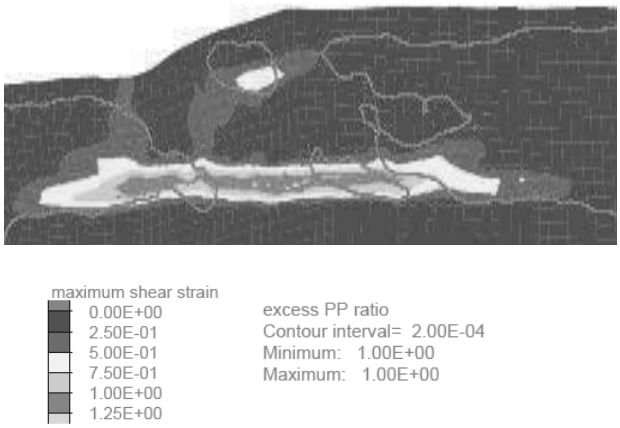

Figure 6. Shear strain contours and excess pore pressure ratio=1 contour at 40 seconds

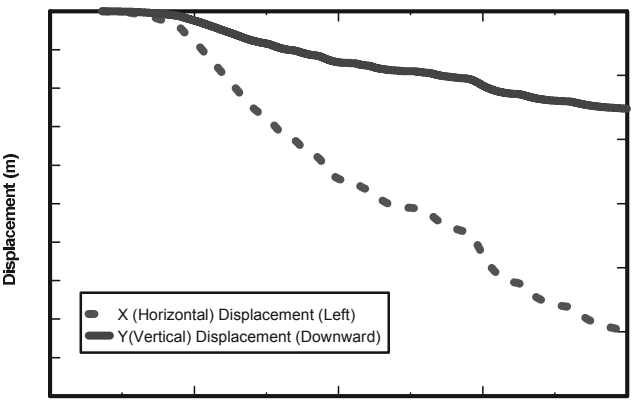

Figure 7. Horizontal (x) and vertical (y) displacement histories at crest of the slope

3 DEBRIS FLOW RUN-OUT DISTANCE

After the development of liquefaction and failure surface in the slope, debris flow can be triggered and the remolded mass during initial failure travels further downslope until the initial stored potential energy is dissipated by friction.

The debris flow run-out distance can be estimated using one- or two- dimensional numerical modeling of sediment-laden submarine flow. For this study, the one-dimensional (1-D) model *BING* assuming one phase flow and "constant volume" constraint. The required input for the simulation includes the bed profile over which the debris mass flow, the initial configuration of the pile of debris slurry, rheological parameters describing the debris slurry and numerical parameters to describe spatial and temporal discretization, run duration and

soil viscosity (Imran and Parker, 2001& 2001). The Herschel-Bulkley rheological model is used for the run-out distance prediction. In the absence of laboratory test data, the yield strength τ_y of 1.5 kPa (30 psf) and reference strain rate γ_r of 1/s were adopted using published relationships as shown on Figure 8 based on soil liquidity index LI (Locat and Lee, 2002).

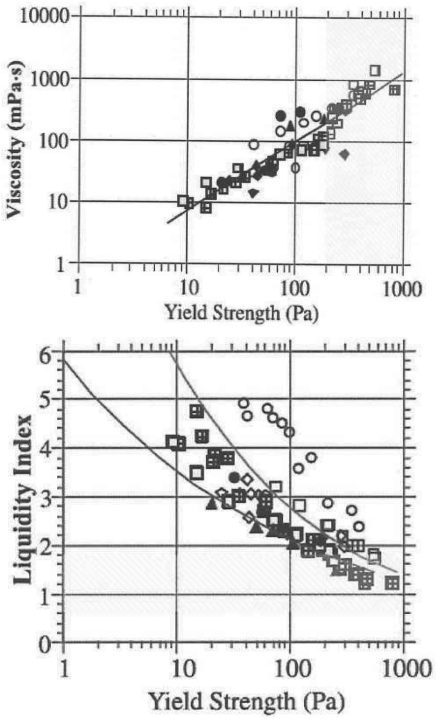

Figure 8. Relationship between yield strength, dynamic viscosity, and soil liquidity index (Reproduced from Locat and Lee, 2002)

Considering debris flow originated at the bottom of the slope and the flow origination mass length of around one-half of the sliding mass length, the estimated run-out distance is around 25 m from the toe of the liquefied slope. These mobilized debris flow mass may pose significant impact force against subsea infrastructure in the flow path, even lead to loss of foundation support.

4 CONCLUSIONS

Dynamic slope instability due to earthquake excitation and subsequent submarine slides can cause mass gravity flow which may cause significant impact force or the loss of foundation support and thus pose great risk for the integrity of offshore structure along the flow path. This paper demonstrated the ability of using a fully coupled nonlinear effective stress analysis to simulate the development of liquefaction and the instability of liquefied slope. The prediction of run-out distance of subsequent debris flow was also discussed here. For practical application, it should be emphasized that the numerical model for assessing the run-out distance should be tested and calibrated with identified historic mass transport deposits (MTD) and geomorphologic conditions along study site.

5 REFERENCES

American Petroleum Institute : Recommended practice for planning, designing and constructing fixed offshore platforms – working stress design, API RP 2A-WSD, twenty-first edition.2000.

International Organization for Standardizatin : *ISO* 19902- Petroleum and natural gas industries- fixed steel offshore structures, DIS version. 2004.

Imran J. and Parker J. 2001. BING, Subaqueous and subaerial finite source debris flow model.

ITASCA Consulting Group Inc. (2012). FLAC- Fast Lagrangian Analysis of Continua Dynamic Analysis.

Kuhlemeyer, R.L., and J.Lysmer. "Finite Element Method Accuracy for Wave Propagation Problems," J.Soil. Mech. & Foundations, Div., ASCE, 99 (SM5), 421-427, May 1973.

Kulhawy, F.H. and Mayne, P.H. 1990. Manual on estimating soil properties for foundation design. Electric Power Research Institute, EPRI.

Locat, J. and Lee H. 2002. Submarine landslides: advanced and challenges, Canadian Geotechnical Journal, No. 39, 193-212.

Mejia, L.H. and Dawson, E.M. 2006. Earthquake Deconvolution for FLAC. FLAC and numerical modeling in geomechanics Proceedings of the 4th international FLAC symposium, Madrid, Spain.